



## Article

# A New Framework to Model Hydraulic Bank Erosion Considering the Effects of Roots

Eric Gasser <sup>1,2,\*</sup>, Paolo Perona <sup>3</sup>, Luuk Dorren <sup>1,2</sup> , Chris Phillips <sup>4</sup>, Johannes Huebl <sup>2</sup>  and Massimiliano Schwarz <sup>1</sup>

<sup>1</sup> School of Agricultural, Forest and Food Sciences, Bern University of Applied Sciences, Laenggasse 85, 3052 Zollikofen, Switzerland; luuk.dorren@bfh.ch (L.D.); massimiliano.schwarz@bfh.ch (M.S.)

<sup>2</sup> Department of Civil Engineering and Natural Hazards, University of Natural Resources and Life Sciences Vienna (BOKU), Peter-Jordan-Strasse 82, 1190 Vienna, Austria; johannes.huebl@boku.ac.at

<sup>3</sup> School of Engineering, The University of Edinburgh, Mayfield Road, Edinburgh EH9 3JL, UK; Paolo.Perona@ed.ac.uk

<sup>4</sup> Manaaki Whenua Landcare Research, P.O. Box 69040, Lincoln 7640, New Zealand; PhillipsC@landcareresearch.co.nz

\* Correspondence: eric.gasser@bfh.ch

Received: 17 February 2020; Accepted: 19 March 2020; Published: 22 March 2020



**Abstract:** Floods and subsequent bank erosion are recurring hazards that pose threats to people and can cause damage to buildings and infrastructure. While numerous approaches exist on modeling bank erosion, very few consider the stabilizing effects of vegetation (i.e., roots) for hydraulic bank erosion at catchment scale. Taking root reinforcement into account enables the assessment of the efficiency of vegetation to decrease hydraulic bank erosion rates and thus improve risk management strategies along forested channels. A new framework (BankforNET) was developed to model hydraulic bank erosion that considers the mechanical effects of roots and randomness in the Shields entrainment parameter to calculate probabilistic scenario-based erosion events. The one-dimensional, probabilistic model uses the empirical excess shear stress equation where bank erodibility parameters are randomly updated from an empirical distribution based on data found in the literature. The mechanical effects of roots are implemented by considering the root area ratio (RAR) affecting the material dependent critical shear stress. The framework was validated for the Selwyn/Waikirikiriri River catchment in New Zealand, the Thur River catchment and the Sulzigraben catchment, both in Switzerland. Modeled bank erosion deviates from the observed bank erosion between 7% and 19%. A sensitivity analysis based on data of vertically stable river reaches also suggests that the mechanical effects of roots can reduce hydraulic bank erosion up to 100% for channels with widths < 15.00 m, longitudinal slopes < 0.05 m m<sup>-1</sup> and a RAR of 1% to 2%. The results show that hydraulic bank erosion can be significantly decreased by the presence of roots under certain conditions and its contribution can be quantified considering different conditions of channel geometry, forest structure and discharge scenarios.

**Keywords:** bank erosion; hydraulic bank erosion; modeling; effects of vegetation; root reinforcement

## 1. Introduction

Floods and windstorms cause about one third of the total economic losses related to natural hazards worldwide [1]. Globally, no other natural hazard occurs as frequently as floods [2]. An important physical process related to floods is hydraulic bank erosion, i.e., the detachment and entrainment of streambank material due to hydrodynamic forces [3]. Hydraulic bank erosion affects sediment dynamics [4,5], disrupts aquatic and sub-aquatic ecosystems [6], decreases channel conveyance [7] and

acts as transport medium for pollutants enriching water bodies with minerals and nutrients affecting the ecosystem through eutrophication [8]. In populated areas, hydraulic bank erosion resulting in undercutting of streambanks in combination with streambank failure represents a significant hazard to agriculture, infrastructure and navigation delivering high quantities of sediment [9]. Further, streambank retreat can cause large wood (LW) recruitment, subsequent entrainment and mobilization of LW. This ultimately adds to the severity of floods, exacerbating damage near civil structures and in urbanized areas [10–15].

It is acknowledged that riparian vegetation, or vegetation growing on and adjacent to streambanks, islands and bars, (1) reduces sediment mobilization due to increases in material strength as well as flow velocity (and thus hydraulic shear stress) [16–18], (2) decreases water pollution [19,20], (3) acts as water temperature regulators [21] and (4) in-stream wood provides habitat for microbial decomposers, creating moist microsites and fish-friendly environments by forming pools and riffles that improve biodiversity [22–24]. Riparian vegetation is therefore important because of its multifunctionality to the wider ecosystem. However, guidelines for the use of vegetation in river restoration projects or forest and channel management to ensure streambank stability and accelerate recovery of streambank and floodplain vegetation are scarce [25]. Modeling the effects of vegetation (i.e., roots) for governing processes affecting streambank stability enables the assessment of how roots stabilize streambanks and decrease erosion without impacting the ecological and geomorphic functionality of the riparian vegetation. Further, quantifying where and how roots could reduce the susceptibility of streambank erosion would allow a better assessment and prioritization of erosion control measures at catchment scale.

Hydraulic bank erosion, in combination with geotechnical bank erosion, is responsible for streambank retreat and is commonly modeled using the empirical excess shear stress equation for cohesive materials [26,27]. The excess shear stress equation describes the rate of sediment removal due to applied hydraulic shear stress in excess of the critical, material-dependent shear stress. However, hydraulic bank erosion is highly complex and is influenced by numerous factors at different spatiotemporal scales. These include (1) the continuous change of the channel hydrogeomorphology pre, post and during erosion events [9,28], (2) the heterogeneity of geotechnical streambank properties for overall bank stability (i.e., cohesion, friction angle, porosity [29]), (3) weathering processes enhancing streambank erodibility [30,31], (4) the presence of roots (i.e., different root densities dependent on vegetation type [32–34]), (5) fluctuating flow properties such as magnitude, duration, event peak and variability [35] and (6) spatiotemporal distribution of precipitation affecting (2) and (5). In theory, all these factors should be considered for bank erosion models at catchment scale, which is why many numerical models require high levels of site-specific parametrization [36].

Riparian vegetation affects the flow regime and the rate of hydraulic bank erosion by (1) increasing streambank resistance and critical shear stress [37,38], and (2) reducing flow velocity at the streambank interface by increasing channel roughness provoking flow energy dissipation through plant deformation [39,40]. One approach to implement the mechanical effects of roots (i.e., root reinforcement) on hydraulic bank erosion in modeling is by adapting critical shear stress. Little quantitative information on how roots affect critical shear stress exists [38,41–43], exacerbating its implementation. Further, the degree of protection depends on the location, root depth and species composition [16,33,44,45]. Models that consider the effects of roots on streambank erosion processes exist (see Table 1), but they emphasize either the geotechnical aspects and use hydrodynamic models to estimate hydraulic properties (e.g., coupling it to a hydrodynamic model at the scale of a river reach, often requiring high levels of parametrization), or they consider the effects of roots by multiplying the critical shear stress by a coefficient.

As a consequence, a relatively simple framework to model hydraulic bank erosion requiring few input parameters to perform and which considers the mechanical effects of roots explicitly and quantitatively was developed. The framework titled BankforNET compiles various approaches to model the susceptibility of hydraulic bank erosion for trapezoidal cross sections. The effects of roots are

considered by adapting the material dependent critical shear stress based on a linear relationship of root density. As such, critical shear stress values do not remain static but are dynamic, depending on the three-dimensional root density distribution.

**Table 1.** Examples of existing bank erosion models that consider the stabilizing effects of roots.

Model Name	Modeled Process	Effects of Vegetation	Reference
BSTEM & RipRoot	Geotechnical bank erosion, hydraulic bank erosion	Root reinforcement by adapting apparent cohesion (geotechnical bank erosion), adaptation of critical shear stress (hydraulic bank erosion) based on values found in literature	[17,34,46–48]
CONCEPTS & REMM	Geotechnical bank erosion, hydraulic bank erosion	Root reinforcement by adapting apparent cohesion (geotechnical bank erosion)	[45,49–52]
SWAT	Hydraulic bank erosion, bed erosion	Adapting critical shear stress based on an empirical effect	[53–55]
	Geotechnical bank erosion	Root reinforcement by adapting apparent cohesion	[44]
SedNet	Hydraulic bank erosion	Consideration of vegetation cover (extent of vegetation cover) using a vegetation factor	[56,57]
	Hydraulic bank erosion	Consideration of vegetation cover (extent of vegetation cover) using a vegetation factor	[36]

This article outlines the first step of this new framework. The objectives of this article are specifically (1) to present the new, probabilistic one-dimensional event-based model that considers the mechanical effects of roots (i.e., root density) and intrinsic randomness that characterizes the Shields entrainment parameter on hydraulic bank erosion for individual cross sections and at catchment scale, (2) to validate the performance of the framework considering three case studies, and (3) to analyze the sensitivity of the modeled results to different parameters.

## 2. Material and Methods

### 2.1. Description of the Framework

We assume a simple working framework in order to limit model complexity and the number of parameters. The erosion rate  $\varepsilon$  ( $\text{m s}^{-1}$ ) at the streambank toe is modeled using the excess shear stress equation [9,26,27,29,58]:

$$\varepsilon = k_d \left( \tau_a - \tau_{c, \text{veg}} \right)^a \quad \text{for } \tau_a > \tau_{c, \text{veg}}, \quad \text{otherwise } \varepsilon = 0 \quad (1)$$

where  $k_d$  is an erodibility coefficient ( $\text{m}^3 \text{N}^{-1} \text{s}^{-1}$ ),  $\tau_a$  is the boundary shear stress applied by the flow (Pa) at the streambank assuming the cross section is trapezoidal,  $\tau_{c, \text{veg}}$  is critical shear stress considering the mechanical effects of roots (Pa) and  $a$  is a dimensionless empirically derived exponent. It is usually assumed that  $a$  takes values close to 1 [27,59].  $k_d$  can be estimated as:

$$k_d = c \tau_{c, \text{veg}}^{-0.5} \quad (2)$$

where  $c$  is a coefficient usually ranging between 0.1 and 0.2 for cohesive material. Since BankforNET uses the excess shear stress equation to calculate erosion rates not only for cohesive but also for noncohesive material,  $c$  is adapted empirically based on  $\tau_a$  and median particle diameter  $D_{50}$  (mm) for noncohesive material. Mean applied hydraulic shear stress [3,46] considering mean bend radius  $r$  (m) assuming uniform flow is calculated as [60]:

$$\tau_a = \begin{cases} \rho_f g R_h S & \text{if } r \text{ is infinite (straight reach)} \\ 2.65 \rho_f g R_h S \left[ \frac{r}{b} \right]^{-0.5} + \rho_f g R_h S & \text{if } r \text{ is finite} \end{cases} \quad (3)$$

where  $\rho_f$  is fluid density ( $\text{kg m}^{-3}$ ),  $g$  is the gravitational acceleration ( $9.81 \text{ m s}^{-2}$ ),  $R_h$  is the hydraulic radius (m),  $S$  is mean channel slope ( $\text{m m}^{-1}$ ) and  $\bar{b}$  is mean channel width (m).  $R_h$  is derived using the Gauckler–Manning–Strickler equation, where Strickler's roughness coefficient is derived empirically as a power function of  $D_{50}$  (mm) for every cross section. To characterize the erodibility of streambank material, critical material dependent shear stress  $\tau_c$  (Pa) is estimated using Shields criterion [61,62]. Rearranging the equation, critical shear stress can be formulated as:

$$\tau_c = \theta [(\rho_s - \rho_f)g D_{50}] \quad (4)$$

where  $\theta$  is the dimensionless Shields entrainment parameter,  $\rho_s$  is solid density ( $\text{kg m}^{-3}$ ) and  $D_{50}$  is median grain size (m). Reported values of  $\theta$  scatter between 0.012 and 0.3 [62] and are divided into classes based on the particle size classification.  $\theta$  hereby defines the threshold at which sediment particles are at incipient motion for noncohesive materials [3], but this approach has also been applied for cohesive materials in few cases [63]. As  $\theta$  depends on the sediment diameter, it can be classified based on measured  $D_{50}$  values. Depending on  $D_{50}$ , BankforNET uses a fitted normal distribution function to determine random values of  $\theta$  (Figure 1) within the range of permissible  $\theta$  values for each particle size class, where the upper and lower threshold are based on values found in the literature [3,38,62,64,65]. For example, if we have coarse gravel (with  $D_{50} = 27 \text{ mm}$ , as presented in Figure 1), the lower and upper permissible threshold of  $\theta$  range from 0.044 to 0.052 based on this defined particle size class [64]. During the iteration process, 10,000 possible values for  $\theta$  are randomly generated considering a normal probability distribution. The mean value is defined as a function of  $D_{50}$  and the standard deviation of the normal distribution is defined based on the particle size class and the corresponding upper and lower threshold for  $\theta$ . Subsequently, 10,000 possible  $k_d$  values are computed resulting in a total of 10,000  $\varepsilon$  values. The final modeled erosion rate then represents the mean cumulative erosion computed from all 10,000 iterations. Although we are not aware of any comprehensive data collection for the characterization of the distribution, the implementation of a normal probability distribution for a permissible and feasible range of  $\theta$  is important to emphasize how the modeled results are influenced by the estimation of  $\theta$ .

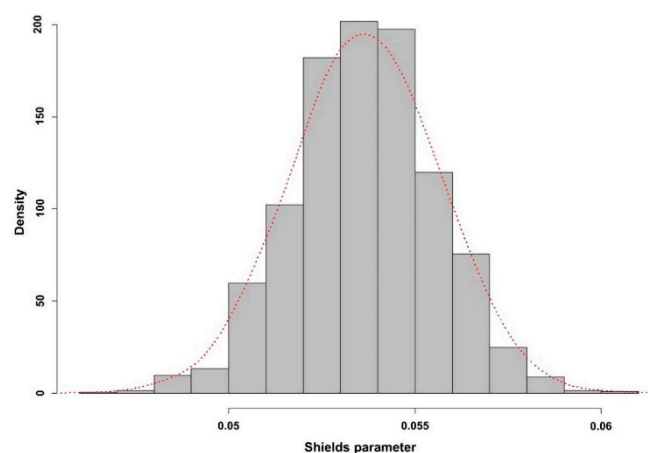


**Figure 1.** Example of the modeled Shields entrainment parameter  $\theta$  distribution for coarse gravel ( $D_{50} = 27 \text{ mm}$ ). The red dotted line represents the fitted density line of the distribution and the y-axis (density) refers to the amount of modeled  $\theta$  used for all 10,000 iterations to model  $\tau_c$ ,  $k_d$  and subsequent  $\varepsilon$ .

The mechanical effects due to the presence of roots in the soil are implemented as an additional term in the estimation of  $\tau_c$ . The modified critical shear stress including the effects of roots  $\tau_{c, \text{veg}}$  is calculated using the root area ratio (RAR). The RAR is the ratio of total root cross sectional area divided by the total area of the soil profile in which the plant grows [66]. Adapting the equation proposed by Pasquale and Perona [42],  $\tau_{c, \text{veg}}$  is calculated as:

$$\tau_{c, veg} = \begin{cases} \tau_c & \text{if } RAR = 0 \\ \tau_c + [a (RAR V_s) + b] & \text{if } RAR > 0 \end{cases} \quad (5)$$

where  $a = 3 \times 10^{-4}$ ,  $b = 9 \times 10^{-3}$  and  $V_s = 2.4$  represents the soil volume of the plot that was used to calibrate the equation [42]. The work from Pasquale and Perona [42] studied the effects of roots on streambed erosion and found that local hydrodynamic bed shear stress conditions when exceeding some critical value gradually cause erosion. This can ultimately lead to uprooting and subsequent entrainment of vegetation. The change in local hydrodynamic bank shear stress conditions also causes streambank erosion when the critical value is exceeded. Even though the uprooting and entrainment process for roots situated on the bed or the streambank may be different, we assume that the effects of roots affecting critical shear stress are the same for both processes.

Measuring RAR in the field is a time-consuming task. Since BankforNET is intended to rapidly assess areas at risk of hydraulic bank erosion considering the effects of roots, RAR is estimated using an adapted root distribution model presented in Schwarz et al. [67], additionally considering vertical root density as proposed by Tron et al. [68]. The root distribution model uses tree stem diameter at breast height (DBH) to estimate root density and maximum rooting distance from the tree stem. The essential root diameters are calculated for each distance from a tree as an upper boundary for root diameter distribution. The number of roots and the values of fine and coarse roots are calculated based on empirical root distribution data. In this framework, empirical root distribution data of white alder (*Alnus incana* L. [69]) was used because this is the only riparian species for which the root distribution model was calibrated. DBH of the four trees were 8.5 cm, 10.0 cm, 7.5 cm and 8.0 cm, respectively. Fine root density  $D_{roots}$  ( $\text{m m}^{-2}$ ) is then calculated as:

$$D_{roots} = \frac{\frac{N_{roots\_tot}}{d_{stem}} d_{stem\ max} - d_{stem}}{(2 \pi d_{stem}) d_{stem\ max}} \quad (6)$$

where fine roots have diameters smaller than 1.5 mm,  $N_{roots\_tot}$  are the total number of fine roots per diameter class using the pipe theory approach,  $d_{stem}$  is the horizontal distance (m), or elongated position from the tree stem at which root density is calculated for, and  $d_{stem\ max}$  is the maximum lateral extent of the root system (m). The estimation of root frequencies with diameters greater than 1.5 mm is done by using a gamma function as presented in Schwarz et al. [67]. The sum of the roots' surface area per diameter class at position  $d_{stem}$  is then divided by the area plot.

The vertical distribution of RAR and subsequent rooting depth is implemented using an analytical approach presented in Tron et al. [68]. The vertical distribution of root density on streambanks and subsequent rooting depth is estimated considering fluctuations of the ground water table, where the ground water table is assumed to be equal to the modeled flow stage. The vertical profile of roots enables the assessment of potential rooting depth and root density. Combining root distribution, vertical root density and rooting depth, RAR values can be estimated for a vertical profile (Figure 2) based on the distance of the tree stem away from the streambank/water interface and the DBH. Figure 2 shows how the presented framework estimates a vertical RAR profile for white alder at six lateral (radial) positions from the tree stem with a DBH of 36 cm.

Reported RAR values range from 0.0002% up to 6.64% depending on tree species, site-specific development of root systems (e.g., lithology) and natural variability of vegetation properties (i.e., age, health [18,66,70–72]). To account for the effects of roots and to compare modeled erosion with and without roots, three RAR values were chosen for the sensitivity analysis;  $RAR = 0.1\%$ ,  $RAR = 1\%$  and  $RAR = 2\%$ . The selection of these three RAR classes seems appropriate if we assume that tree stems are between 0.50 m and 2.50 m away from the streambank/water interface. After the determination of  $\tau_{c, veg}$ ,  $\varepsilon(t)$  is integrated over the duration of the discharge event  $T$  (min) to calculate the cumulative erosion  $E$  (m) at the streambank toe:

$$E = \int_0^T \varepsilon(t) dt \quad (7)$$

Since 10,000  $\varepsilon$  values are computed, average cumulative erosion is calculated and used as the final modeled cumulative erosion. Additionally, mean channel width is adapted iteratively based on the modeled erosion for every time step. Therefore, the final average cumulative erosion is based on a continuous adaption of the bank width. Figure 3 illustrates conceptually how BankforNET models hydraulic bank erosion in one dimension at the toe of the streambank considering the effects of roots. Hydraulic bank erosion at the streambank toe decreases the resisting forces that prevent the streambank from failure. Assuming that the undercutting of streambanks eventually leads to failure, this framework allows practitioners to assess the susceptibility of hydraulic bank erosion and subsequently areas at risk of streambank retreat.

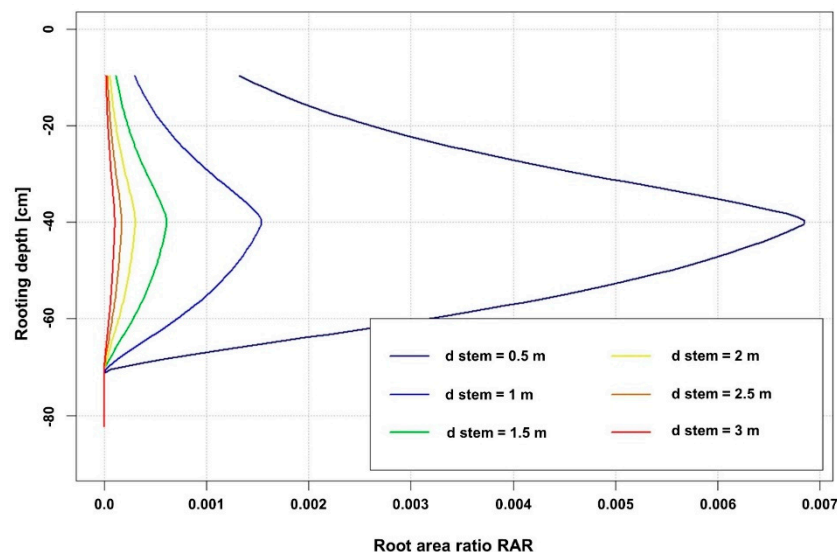


**Figure 2.** Modeled mean root area ratio (RAR) distribution of white alder (*Alnus incana* L.) in a modeled vertical profile at six lateral (radial) positions from the tree stem ( $d_{\text{stem}} = 0.5$  m, 1.0 m, 1.5 m, 2.0 m, 2.5 m and 3.0 m) with a DBH of 36 cm. Maximum modeled rooting depth was 74 cm. Note that the integral of the RAR distribution in vertical direction equals the mean RAR per total surface of the plot at six lateral (radial) positions.

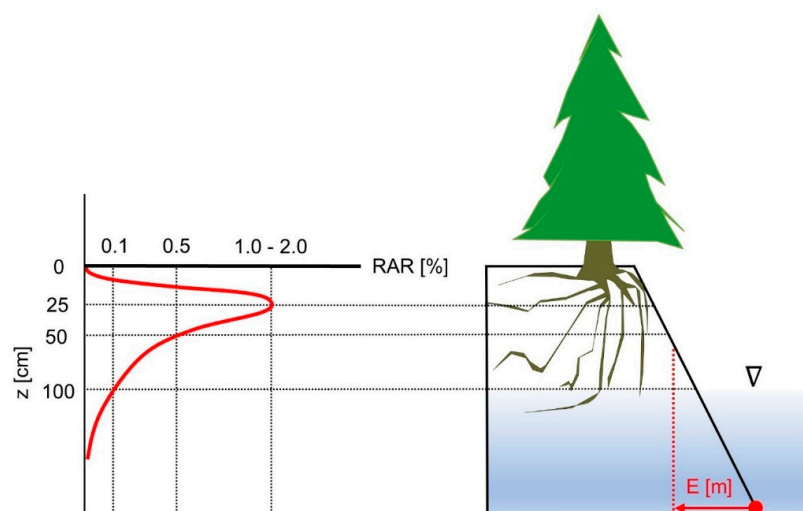


**Figure 3.** Conceptual illustration of how BankforNET models hydraulic bank erosion considering RAR. The density of the RAR is a function of rooting depth and roots protecting the streambank affected by the flow. On the left is a conceptual illustration of root density (i.e., RAR) as a function of rooting depth. The red dot and arrow on the right represent the one-dimensional erosion at the bank toe that is modeled by BankforNET considering the vertical RAR distribution if roots are present.



If no discharge data is available, peak discharge  $Q_{max}$  ( $\text{m}^3/\text{s}$ ) for different return periods is estimated based on a modified and adapted empirical relation proposed by Kölla [73]:

$$Q_{max} = [\ln(RP) + 6.38] A_c^{0.61} \quad (8)$$

where  $RP$  is the return period (year) and  $A_c$  is the catchment area ( $\text{km}^2$ ). The function in brackets substitutes rainfall intensity in the equation from Kölla [73] for different scenarios (return periods) and was established based on observed data. The presented empirical equation was developed specifically for this model framework and was calibrated using observed precipitation and discharge data.

Event duration  $T$  (min) is then also estimated empirically based on data from Marchi et al. [74], defining the duration of the discharge event as a power function of catchment area ( $\text{km}^2$ ):

$$T = 298 A_c^{0.355} \quad (9)$$

In BankforNET, a triangular shape is used to represent the hydrograph, as proposed by the US soil conservation service (SCS) [75]. This approach allows the framework to be applicable for multiple catchments without calibration of the hydrograph.

## 2.2. Case Studies

### 2.2.1. The Selwyn/Waikirikiriri River Catchment

Stecca et al. [28] presented a framework for the analysis of noncohesive hydraulic bank erosion algorithms. In their article, they assessed the performance of different “candidate” hydraulic bank erosion models by applying the different models to a case study: The Selwyn/Waikirikiriri River flows southeast from the foothills of the Southern Alps in the South Island of New Zealand into Lake Ellesmere/Te Waihora ( $43^\circ 30' 18''$  S,  $171^\circ 58' 54''$  E). In 2008, a single flood event with a duration of 38.9 h, where the river was morphologically active, peak discharge of  $\sim 130 \text{ m}^3 \text{ s}^{-1}$  occurred. During this event, the right streambank at an investigated cross section experienced 15.00 m of retreat. Based on a pre- and post-flood digital elevation model (DTM), the models were tested (Table 2). The duration of the modeled hydrograph was reduced to 38.9 h; during this time the river was morphologically active. BankforNET needs few input parameters which are provided by Stecca et al. [28], except for mean bank angle. Mean bank angle is assumed to be  $85^\circ$  based on the preflood survey terrain analysis. Based on the information provided by Stecca et al. [28], BankforNET was validated to estimate how reliably it can predict hydraulic bank erosion without considering the effects of roots as both streambanks were not covered by vegetation.

**Table 2.** Input parameters to perform BankforNET based on the analysis presented in Stecca et al. [28].

Input Parameters	Symbol	Dimension	Value
Discharge	Q	$\text{m}^3 \text{ s}^{-1}$	130
Duration of flood event	t	h	38.9
Mean channel width	W	m	62
Mean channel slope	S	$\text{m m}^{-1}$	0.007
Mean streambank angle	BA	$^\circ$	85
Mean bend radius	R	m	185
Median sediment diameter	D50	mm	27
Root area ratio	RAR	%	-

### 2.2.2. The Thur River Catchment

Data of a cross section of the river Thur in Niederneunforn in the Canton of Thurgau, Switzerland ( $47^\circ 35' 37''$  N,  $8^\circ 46' 00''$  E) was used for further validation of BankforNET. The river Thur has a catchment area of  $1601 \text{ km}^2$  at the observed cross section. Dense vegetation (mature trees) cover the streambanks

on both sides. During the hydrological year 2010, impressive retreat of approximately 50 m on the right streambank (cut bank) occurred [76]. The input parameters (Table 3) for BankforNET are based on reported data [77–79]. The erosion events were selected based on discharge data provided by the Swiss Federal Office for the Environment (FOEN) [80], where the monthly maximum discharge was used for 12 events representing each month from the hydrological year 2010 (Table 4). Since no event lasted longer than one day, the discharge duration was modeled to be 24 h. For each erosion event, we assumed that the input parameters remained the same except for discharge and the adaption of channel width due to the erosion of the previous erosion event because no information on how the other parameters changed during the erosion events was found in the literature.

**Table 3.** Input parameters for the cross section at the Thur River catchment in Canton of Thurgau, Switzerland. Discharge (Q) for the 12 scenarios (events) are presented in Table 4.

Input Parameters	Symbol	Dimension	Value
Discharge	Q	$\text{m}^3 \text{s}^{-1}$	see Table 4
Duration of each flood event	t	h	24
Mean channel width	W	m	30
Mean channel slope	S	$\text{m m}^{-1}$	0.0016
Mean streambank angle	BA	°	45
Mean bend radius	R	m	100
Median sediment diameter	D50	mm	10
Root area ratio	RAR	%	0.1/1/2

**Table 4.** Discharge (Q) scenarios (events) for the Thur River catchment in Canton of Thurgau, Switzerland.

Event		1	2	3	4	5	6	7	8	9	10	11	12
Q	$\text{m}^3 \text{s}^{-1}$	122	206	362	174	120	170	61.9	340	501	390	492	628

The effects of roots for different discharge scenarios were also modeled for the Thur River. Based on flood statistics, discharge scenarios for return periods (RP) of 2 years ( $HQ_2 = 576 \text{ m}^3 \text{s}^{-1}$ ), 5 years ( $HQ_5 = 827 \text{ m}^3 \text{s}^{-1}$ ), 30 years ( $HQ_{30} = 952 \text{ m}^3 \text{s}^{-1}$ ), 100 years ( $HQ_{100} = 1068 \text{ m}^3 \text{s}^{-1}$ ) and 300 years ( $HQ_{300} = 1158 \text{ m}^3 \text{s}^{-1}$ ) were used to model erosion scenarios and to quantify relative cumulative erosion reduction for three RAR classes of 0.1%, 1% and 2%. The streambank height of the Thur River catchment was approximately 3.5–4.0 m and therefore, observed effects of roots were negligible under current conditions. However, it is possible that under different conditions (e.g., decreased discharge for longer time periods), roots grow deeper, and root distribution will reach higher values at the streambank toe. Under these hypothetical but realistic conditions, the magnitude of the effects of roots for five different return periods were calculated. While the observed effects of roots on reducing the susceptibility of hydraulic bank erosion were negligible under current conditions, it is possible that if the water level drops and remains low over longer time periods, roots penetrate to deeper depths to reach the water table [68]. Roots would then have a significant effect on reducing the susceptibility to hydraulic bank erosion.

### 2.2.3. The Sulzigraben Catchment

To validate the framework at a cross section where roots were present, a profile in the Sulzigraben catchment was investigated (46°46′00″ N, 7°48′52″ E). The Sulzigraben is a mountain creek in the Canton of Bern, Switzerland and a small tributary of the river Zulg with a total catchment area of 5.02 km<sup>2</sup>. In 2012 and 2015, peak discharge caused noticeable hydraulic and geotechnical bank erosion triggering sediment mobilization as well as LW recruitment and transport [81]. No hydrographic recording station is installed in the Sulzigraben, but during the 2012 and 2015 events, precipitation intensities were reconstructed based on meteorological radar data. Precipitation intensities were



approximately  $60 \text{ mm h}^{-1}$  to  $100 \text{ mm h}^{-1}$  for the 2012 event, and  $100 \text{ mm h}^{-1}$  to  $160 \text{ mm h}^{-1}$  for the 2015 event [81]. To estimate total streambank retreat, a DTM of the year 2012 with a spatial resolution of  $0.5 \text{ m} \times 0.5 \text{ m}$  was used. In 2019, a 2 m wide and 0.8 m deep profile was dug on the left streambank to measure the RAR of a sycamore maple (*Acer pseudoplatanus* L.). The tree stem was standing 2.5 m away from the streambank/water interface with a DBH of 36 cm. Area sectors were defined based on the vertical position of the roots resulting in 5 sectors in depths of 0–15 cm, 15–30 cm, 30–45 cm, 45–60 cm and 60–75 cm. For every sector, roots were counted and individual root diameters were measured. Considering the DTM of 2012, streambank height was approximately 60 cm corresponding to a measured RAR of 1% in 2019. In 2012, the distance of the tree stem to the streambank/water interface was 3.35 m with lower RAR values compared to the ones observed in 2019. The root distribution model was used to calculate changes in the vertical RAR distribution to consider that the streambank/water interface comes closer to the tree stem as the erosion progresses. Further, modeled vertical RAR distribution for white alder was scaled to match those of the investigated vertical RAR distribution of sycamore maple at the Sulzigraben catchment. Roots were present in the left streambank and no roots were present in the right streambank. Subsequently, hydraulic bank erosion for the left streambank was modeled considering the effects of roots and the right streambank was modeled without considering the effects of roots. Further, we assume that the tree present in 2019 was also present in 2012 and that no other trees were standing on or adjacent to the investigated cross section in 2012.

The catchment area is  $2.2 \text{ km}^2$  at the studied cross section. Discharge for both events were estimated using BankforNET considering the precipitation intensities of 2012 and 2015. Other input parameters (Table 5) are based on the field survey from 2019 and estimations using the DTM. Channel and streambank geometries were measured using measuring tape, a double meter stick and a TruePulse 200 laser rangefinder. Channel slope, mean streambank angle and bend radius were similar in 2012 and in 2019. The initial streambank width is based on the 2012 DTM for the first erosion event. For the second erosion event, modeled total erosion of the first event was added to the initial streambank width, increasing the width. Median sediment diameter was measured in the field using the line-by-number analysis [82]. Measured median sediment diameter were assumed to be the same for both erosion events.

**Table 5.** Input parameters for the cross section at the Sulzigraben catchment in the Canton of Bern, Switzerland for the two erosion events.

Input Parameters	Symbol	Dimension	Value
Discharge	Q	$\text{m}^3 \text{ s}^{-1}$	11.4/18.9
Duration of flood event	t	h	6.5
Mean channel width	W	m	4/5
Mean channel slope	S	$\text{m m}^{-1}$	0.07
Mean streambank angle	BA	°	29
Mean bend radius	R	m	$\infty$ (straight reach)
Median sediment diameter	D50	mm	98
Root area ratio	RAR <sub>max</sub>	%	1

### 2.3. Sensitivity Analysis

An overall sensitivity analysis of BankforNET was conducted to quantify the effects of roots on the erosion reduction under different conditions. Two types of datasets were used for the sensitivity analysis: (1) For the three case studies presented in this paper, the input parameters varied by  $\pm 10\%$  from the original value for each model run without considering the effects of roots. Additionally, we repeated the analysis using RAR values of 0.1%, 1% and 2%. (2) Using measured input parameters from 37 study reaches, the susceptibility of streambanks to hydraulic bank erosion considering the effects of roots was calculated. Additional data of 34 study reaches including step-pool, cascade and plane-bed mountain stream reaches from the eastern and western side of the South Island in New

Zealand [83] were included. While detailed information on vegetation, root distribution and erosion rates are missing for most reaches, the 37 study reaches do, conceptually, enable the possibility to use hydraulic geometry relationships to categorize the stabilizing effects of roots.

### 3. Results

#### 3.1. Validation

##### 3.1.1. The Selwyn/Waikirikiriri River Catchment

For the Selwyn/Waikirikiriri River catchment, mean cumulative streambank erosion was modeled to be 17.40 m. The modeled result deviates from the observed values of 15.00 m [28] by +2.40 m, or by 16%. Figure 4 shows the cumulative distribution of modeled bank erosion as a function of event duration and discharge (blue line). The red dashed lines correspond to the modeled erosion results of BankforNET using different Shields parameters based on a fitted normal distribution function defined by  $D_{50}$  and the corresponding particle size class. The upper and lower threshold of the red lines hereby represent upper and lower possible cumulative erosion values considering a probabilistic approach distinguishing  $\theta$  as described in Section 2.1. The black line is mean modeled cumulative erosion based on all modeled erosion iterations. As visualized in Figure 4, streambank erosion seems to occur when discharge is higher than  $11 \text{ m}^3 \text{ s}^{-1}$  and the rate of cumulative erosion increases nonlinearly with increasing discharge.

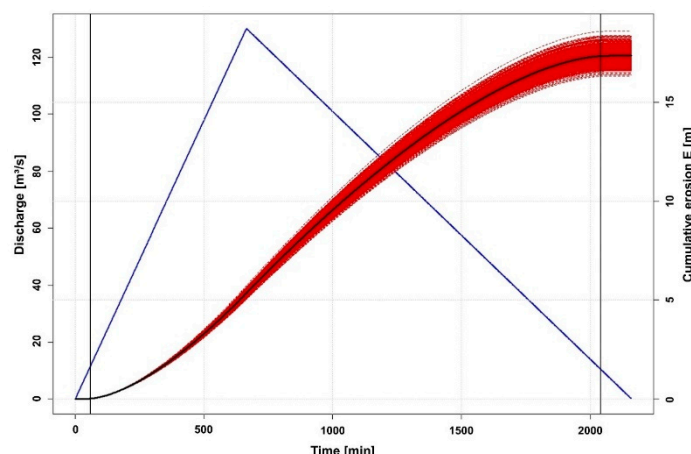


**Figure 4.** Example of the modeled cumulative erosion for the Selwyn/Waikirikiriri River catchment (where no roots were present). The blue line represents the triangular hydrograph, the red lines represent each erosion iteration and the black line represents the mean cumulative erosion (m). The two black vertical lines indicate when erosion is equal to zero (at discharge values  $\leq 11 \text{ m}^3 \text{ s}^{-1}$  for the Selwyn/Waikirikiriri River catchment).

##### 3.1.2. The Thur River Catchment

At the cross section for the Thur River catchment, cumulative streambank erosion of all events (i.e., the sum of mean erosion for the different erosion events) was modeled to be 53.40 m without roots, 52.70 m with a RAR of 0.1%, 46.60 m with a RAR of 1% and 40.30 m with a RAR of 2% (Table 6). Observed erosion for the 2010 season is approximately 50.00 m (Schirmer et al. [76]). The modeled erosion deviates from the observed erosion by +3.40 m, or by 7% without roots, +2.70 m, or by 5% with RAR of 0.1%, −3.40 m or by 7% with RAR of 1% and −9.70 m, or by 19% with RAR of 2%. Since the effects of roots were negligible, modeled erosion deviates from observed erosion by 7%.

**Table 6.** Modeled streambank erosion for the Thur River catchment.

Input Parameters	Symbol	Dimension	Event Number											
			1	2	3	4	5	6	7	8	9	10	11	12
Modeled streambank erosion (no roots)	E	m	1.37	3.20	5.90	2.56	1.32	2.47	0.10	5.58	7.75	6.32	7.64	9.18
Standard deviation	-	m	0.55	1.22	2.16	0.99	0.54	0.96	0.04	2.04	2.76	2.29	2.73	3.23
Modeled streambank erosion (RAR = 0.1%)	E	m	1.32	3.14	5.84	2.50	1.28	2.41	0.08	5.51	7.68	6.25	7.57	9.11
Standard deviation	-	m	0.54	1.20	2.13	0.97	0.52	0.94	0.03	2.02	2.74	2.27	2.71	3.21
Modeled streambank erosion (RAR = 1%)	E	m	0.93	2.61	5.20	2.00	0.89	1.93	0.01	4.90	7.05	5.64	6.95	8.48
Standard deviation	-	m	0.38	1.02	1.94	0.79	0.37	0.77	0.006	1.82	2.54	2.07	2.51	3.01
Modeled streambank erosion (RAR = 2%)	E	m	0.57	2.06	4.58	1.50	0.53	1.44	0.00	4.26	6.37	4.98	6.27	7.78
Standard deviation	-	m	0.25	0.82	1.72	0.61	0.23	0.58	0.00	1.61	2.33	1.86	2.29	2.80

To assess the magnitude of the effects of roots for five different return periods based on available flood statistics, the mean cumulative erosion reduction (%) is calculated for RAR of 0.1%, 1% and 2% (Figure 5). Mean cumulative erosion reduction is hereby the difference between modeled erosion without roots and modeled erosion with roots divided by the modeled erosion without roots.

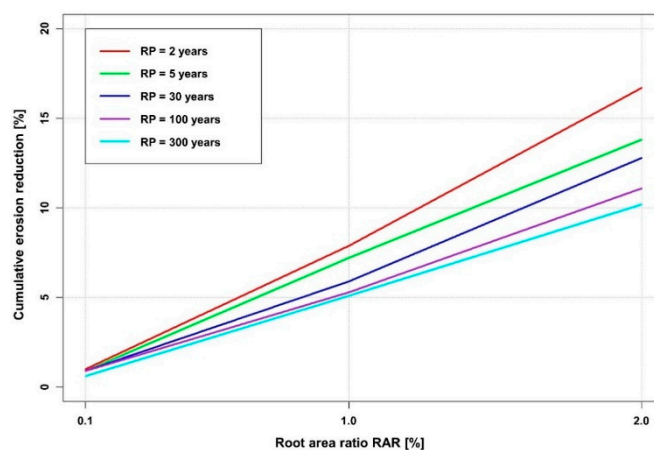
**Figure 5.** Cumulative erosion reduction (%) due to the mechanical effects of roots for return periods (RP) of 2, 5, 30, 100 and 300 years with RAR of 0.1%, 1% and 2% for the Thur River catchment.

Table 7 shows the cumulative erosion reduction considering different RAR values and different discharge scenarios for the Thur River catchment. The results indicate that with increasing event magnitude, the relative effects of roots decrease. With increasing RAR, the susceptibility of streambank erosion decreases due to the presence of roots (see Table 7). In short, with higher RAR and discharge scenarios of lower intensities and smaller return periods, the effects of roots are more distinct. Considering future climate change scenarios, these results are feasible and can become even more relevant considering the effect that climate change exerts on discharge and tree species adaption.

**Table 7.** Cumulative erosion reduction for the Thur River catchment considering different return periods and root area ratios.

Return Period (Year)	RAR (%)	Cumulative Erosion Reduction (%)
2	0.1	1
2	1	8
2	2	17
5	0.1	1
5	1	7
5	2	14
30	0	1
30	1	6
30	2	13
100	0	1
100	1	5
100	2	11
300	0.1	1
300	1	5
300	2	10

### 3.1.3. The Sulzigraben River Catchment

Mean cumulative streambank erosion was modeled to be 0.45 m for the first event and 0.40 m for the second event when the effects of roots are considered (left streambank). Without roots, mean cumulative erosion was modeled to be 0.55 m for the first event and 0.50 m for the second event (right streambank). Total erosion was estimated to be 1.70 m based on the DTM from 2012 and the field survey from 2019. Modeled erosion for both events (with roots for the left streambank and without roots for the right streambank) results in a total of 1.90 m erosion. As such, the modeled results deviate from observed values by +0.20 m, or by 12%. The modeled results also suggest that the cumulative erosion reduction due to the presence of roots for this cross section is 14%. Figure 6 (top) shows the vertical root distribution of measured RAR at measured depths (*Acer pseudoplatanus* L., blue) and modeled vertical RAR distribution at modeled depths for white alder (*Alnus incana* L.), scaled to match the vertical RAR distribution of the investigated sycamore maple RAR distribution (red). To model hydraulic bank erosion for the Sulzigraben catchment using the framework with measured RAR values, the vertical root distribution of white alder scaled to represent the vertical RAR distribution of sycamore maple was used. At depths of 60 cm, RAR changes with values of 0.4% to 1% depending on the distance from the tree stem (Figure 6, bottom). Specifically, in 2012, the RAR at a distance of 3.35 m away from the investigated tree was  $\approx$  0.4% and increased up to 1% during the erosion events to a distance of 2.50 m in 2019 for the left streambank. Simultaneously, streambank width increases while the distance of the tree stem to the streambank/water interface decreases (Figure 6, bottom).

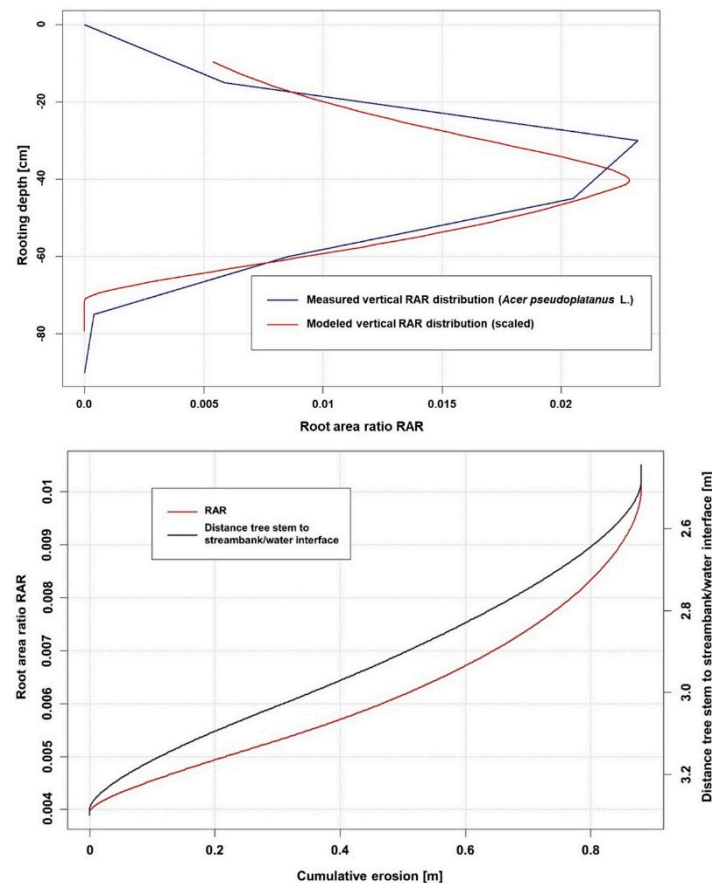


**Figure 6.** Measured vertical RAR distribution for sycamore maple (*Acer pseudoplatanus* L., blue) and modeled vertical RAR root distribution for white alder (*Alnus incana* L.), scaled to represent the measured sycamore maple vertical RAR distribution (red). At the end of both erosion events, the distance of the tree stems to the streambank/water interface was 2.50 m and the DBH was set to 36 cm for both trees (**top**). Modeled RAR for both erosion events at the Sulzigraben catchment considering the adaption of RAR as a function of erosion and the changing distance of the tree stem to the streambank/water interface for the left streambank (**bottom**).

### 3.2. Sensitivity Analysis

Based on the sensitivity analysis presented in Figures 7–9, the parameters that have the greatest influence on the modeled results are in order of importance: Median sediment diameter ( $D_{50}$ ), mean channel slope ( $S$ ), mean bend radius ( $R$ ), mean channel width ( $W$ ) and mean bank angle ( $BA$ ). While the model is least sensitive to changes in bank angle, it was observed that by varying the bank angle between  $1^\circ$  and  $90^\circ$  while all the other input parameters remain unchanged, the greatest differences in the modeled erosion occurred when the bank angle was  $\leq 30^\circ$ . With shallower bank angles, the hypotenuse, or in this case the length of the streambank affected by the flow, is greater than it is for steeper bank angles. Therefore, modeled erosion rates were lower if the bank angle was set to values  $\leq 30^\circ$  as the applied shear stress was distributed over a greater length and was reduced at the point erosion was modeled. With bank angles  $> 30^\circ$ , modeled erosion varied negligibly. Therefore, bank angle has a negligible influence on the results, especially for bank angles  $> 30^\circ$ . The stabilizing effects of roots on hydraulic bank erosion is significantly different for the RAR classes. The stabilizing effects of roots become less obvious with varying channel slope and  $D_{50}$ .

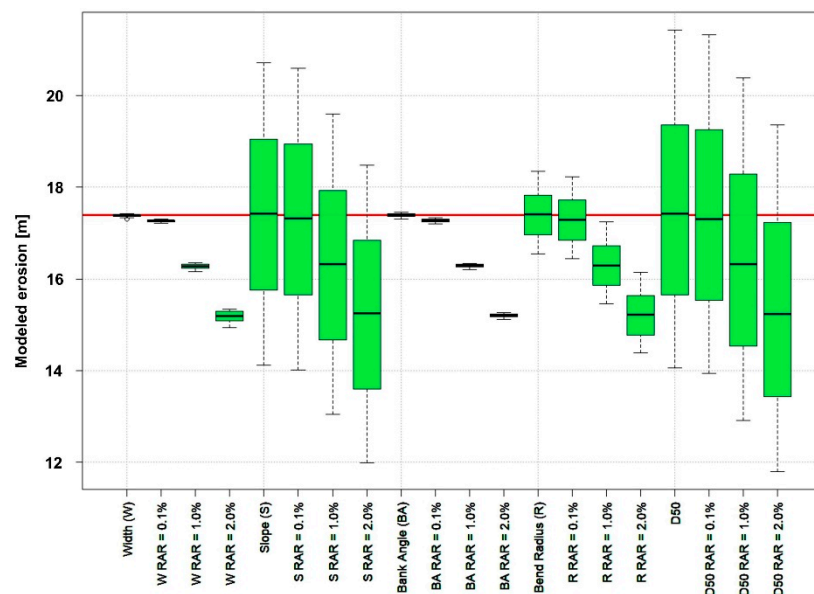


**Figure 7.** Sensitivity analysis using the data for the Selwyn/Waikirikiriri River catchment. For every input parameter, the values varied  $\pm 10\%$  from the original input value. The red line is the reference for the modeled erosion = 17.40 m using the original input values. Each boxplot represents the quantile of the cumulative erosion.

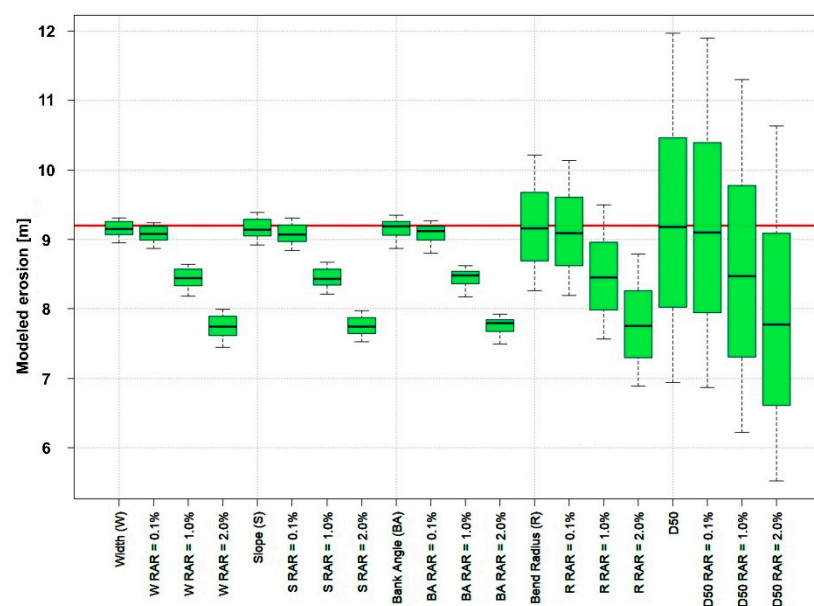


**Figure 8.** Sensitivity analysis representing event 12 for the Thur River catchment. For every input parameter, the value varied  $\pm 10\%$  from the original input value. The red line is the reference for the modeled erosion = 9.18 m using the original input values. Each boxplot represents the quantile of the cumulative erosion.



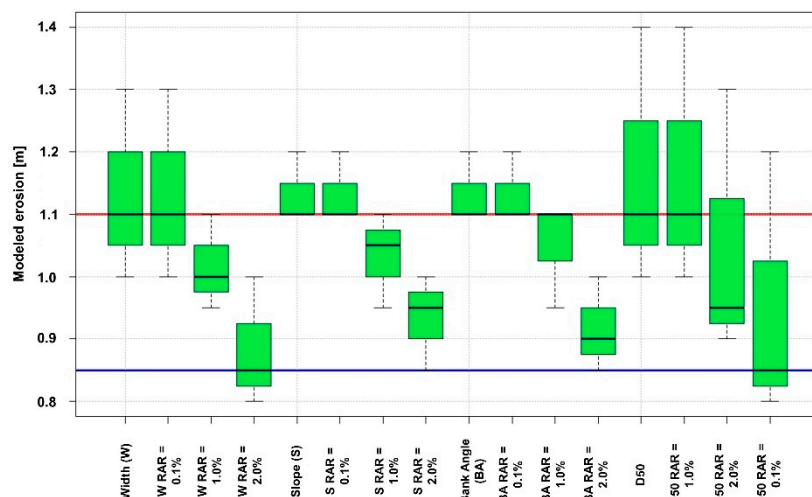


**Figure 9.** Sensitivity analysis for the Sulzgraben catchment for the first erosion event in 2012. For every input parameter, the value varied  $\pm 10\%$  from the original input value. The red line is the reference for the total modeled erosion = 1.10 m for the first event using the original input values without considering the effects of roots. The blue line is the reference for the total modeled erosion = 0.85 m for the first event using the original input values considering the effects of roots (left streambank). Each boxplot represents the quantile of the cumulative erosion.

### 3.3. Susceptibility to Hydraulic Bank Erosion Considering the Effects of Roots

The susceptibility of mean cumulative erosion for the 37 study reaches was modeled for the three RAR classes with a return period of 100 years. The cumulative erosion reduction (%) is presented in relation to channel width and channel slope (Figures 10 and 11). The results suggest that roots have a more significant stabilizing effect for channels with widths  $< 15.00$  m and longitudinal slopes  $< 0.05$  m  $\text{m}^{-1}$ . The cumulative erosion reduction varies between 0% and 60% with a RAR of 0.1%, between 0% and 100% with a RAR of 1.0% and between 2% and 100% with a RAR of 2% under specific channel conditions. The distance of the tree stem to the streambank/water interface was placed at 1.00 m. Relative cumulative erosion reduction of 100% was reached by four different cross sections: At the four cross sections, total modeled absolute erosion reduction was at most 1.04 m and the median sediment diameter was exclusively  $\geq 112$  mm.

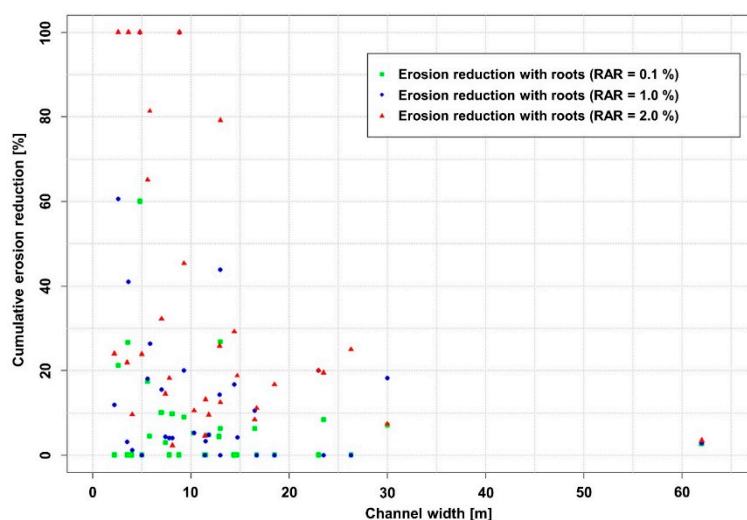


**Figure 10.** Stabilizing effects of roots on hydraulic bank erosion in relationship to channel width. The points represent the cumulative erosion reduction (%) with RAR = 0.1% (green), RAR = 1% (blue) and RAR = 2% (red).

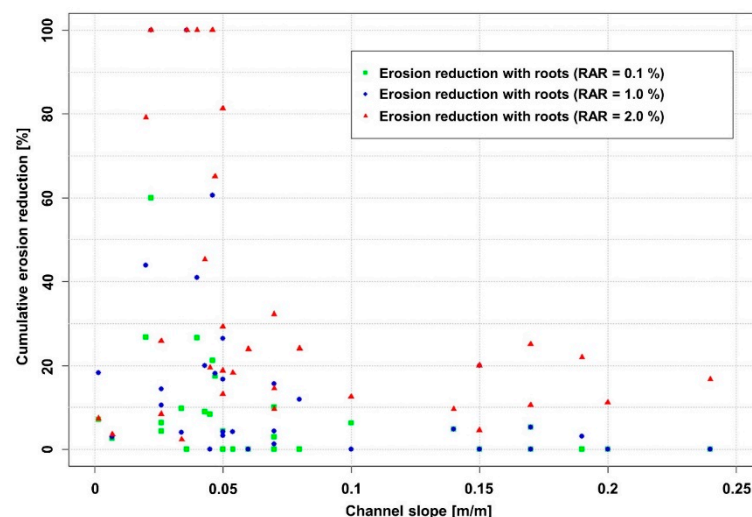


**Figure 11.** Stabilizing effects of roots on hydraulic bank erosion in relation to channel slope. The points represent the cumulative erosion reduction (%) with RAR = 0.1% (green), RAR = 1% (blue) and RAR = 2% (red).

Based on the modeled results of the 37 study reaches in this study, we propose a modified version of the susceptibility matrix presented in Gasser et al. [84] (Figure 12). While the matrix presented in Gasser et al. [84] was based on values found in the literature, the matrix presented in this article was adapted based on the original matrix considering the modeled results. Hereby, the original matrix was adapted to test its validity. The susceptibility matrix shows the stabilizing (positive) effects of roots in relation to channel width and channel slope. The main objective of the matrix is that forest and channel managers can use it to assess the degree of stabilization based on geometric criteria that can be assessed rapidly in the field. Based on the location on the matrix, targeted forest and channel management to reduce the susceptibility of hydraulic bank erosion can be implemented. The matrix is however only valid for streambanks where rooting depth is greater or equal to streambank height. Green areas represent channel conditions (channel width and slope) where roots can significantly reduce hydraulic bank erosion through mechanical root reinforcement. The susceptibility of hydraulic bank erosion can be reduced up to 100% with a RAR of 1% and 2%, representing somewhat best forest conditions for cross sections with specific channel geometries. Yellow areas represent channel conditions where the stabilizing effects of roots are variable, that is the susceptibility of hydraulic bank erosion can be reduced up to 32% with a RAR of 2%. The red area represents the channel conditions where roots have a low or no effect on reducing the susceptibility of hydraulic bank erosion. The grey area is not defined as it is assumed that channels with widths  $> 30.00$  m and longitudinal slopes  $> 0.15 \text{ m m}^{-1}$  are unlikely to exist in nature.

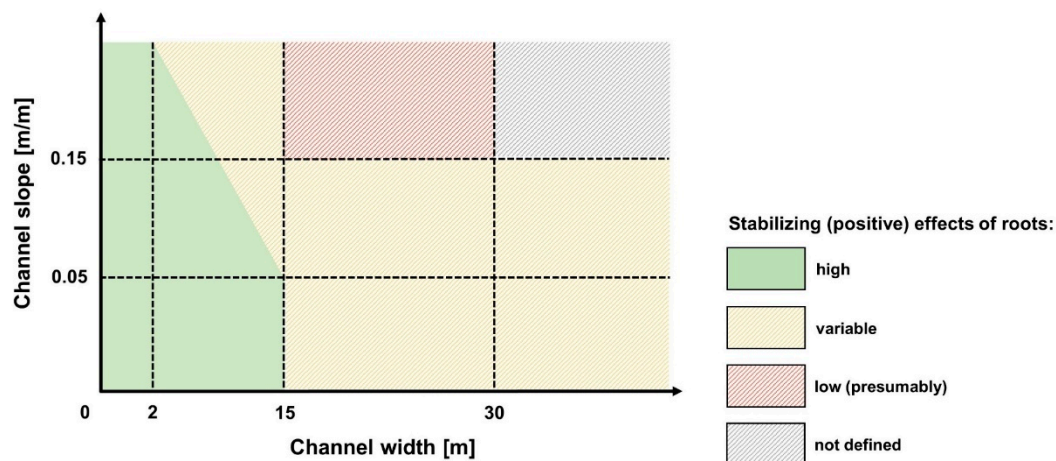


Figure 12. Susceptibility matrix to hydraulic bank erosion highlighting the stabilizing effects of roots.

#### 4. Discussion

Using the excess shear stress equation, modeling errors can occur due to either systematic underestimation of  $\tau_c$  and  $k_d$ , overprediction of the applied shear stress  $\tau_a$ , or that the exponent  $a$  in Equation (1) is not constant [9,35].  $\tau_c$  and subsequent  $k_d$  are estimated by randomly selecting  $\theta$  based on a fitted normal distribution function dependent on median sediment diameter ( $D_{50}$ ) allowing the model to cover a range of permissible  $\theta$  values for the corresponding particle size class. The final result then represents the mean cumulative erosion based on the random selection of  $\theta$  computing 10,000 values for  $E$ , giving information about the potential probability distribution of over- or underestimation. However, since the determination of  $\tau_c$  and  $k_d$  is derived from  $\theta$  based on permissible values found in the literature and not from field tests, a normal distribution is assumed to generate a density function. Measuring  $\tau_c$  values, for example by using a jet-test [27,29,34,58,85,86], would allow the acquisition of site-specific data to parameterize the model resulting in less variation between observed and modeled erosion rates [87]. However, since the variation of the upper and lower threshold of  $\theta$  for every particle size class is not particularly high and  $\theta$  alone does not distinguish  $\tau_c$ , this approach is feasible and based on the results, the effect of potentially misallocated  $\theta$  is marginal. The deviation of the magnitude of  $\tau_a$  was not assessed, because hydraulic shear stress cannot be measured directly in the field. As such, we cannot assess the exact magnitude of  $\tau_a$ , but based on the presented results, modeled  $\tau_a$  and subsequent erosion seem reasonable. BankforNET uses a triangular hydrograph instead of the more commonly used Gamma curve. Based on the approach of a synthetic unit hydrograph, a triangular shape can be used as a uniform hydrograph for multiple catchments. This may not be the most accurate approach in modeling discharge and erosion, but it allows the use of one hydrograph to represent multiple catchments and scenarios keeping the models input parameters simple.

The excess shear stress equation is used to estimate hydraulic bank erosion for cohesive material. Shields criterion was developed for noncohesive materials. Empirically adapting the coefficient  $c$  based on  $\tau_a$  and  $D_{50}$  for noncohesive material enables the use of BankforNET to model hydraulic bank erosion for noncohesive streambanks with  $D_{50}$  of 98 mm, 27 mm and 10 mm with reasonably accurate results. This suggests that the excess shear stress equation can be applied for noncohesive streambanks and Shields criterion for cohesive streambanks, when considering a variability of  $\tau_c$  and an adaption of  $c$ . However, the high model sensitivity to changes in  $D_{50}$  could be a consequence of the deviation from the original development criteria.

Modeled cumulative erosion deviates from the observed erosion by 7% to 19%. At the Sulzigraben catchment, modeled erosion deviates from observed erosion by 12% with measured RAR of 1%. The results suggest that for this catchment, cumulative erosion reduction was 14% due to presence of roots. The results are feasible and suggest that roots have a significant effect on reducing the susceptibility of hydraulic bank erosion. Using the root distribution model [67] considering root density in vertical

direction [68] allows BankforNET to estimate a vertical RAR profile. Comparing modeled rooting depths to actual rooting depths, the model predicts the vertical extent of roots with reasonable accuracy. While the modeled RAR using data of white alder lies within the range of reported RAR values, it is considerably smaller than the measured RAR for sycamore maple at the Sulzigraben catchment. To validate the model using a measured vertical RAR distribution, the values of the calibrated model were scaled to represent the measured values of sycamore maple. Better parametrization, calibration and testing for different tree species under different soil conditions is however still needed.

The sensitivity analysis shows that the modeling framework is most sensitive to changes in  $D_{50}$  and channel slope. While the sensitivity to changes in mean channel width and mean streambank angle are rather small, changes in mean bend radius have a smaller influence on the modeled results. The range of modeled erosion by varying the input parameters with  $\pm 10\%$  depends on the absolute value of the input parameter. For the Selwyn/Waikirikiriri River catchment, mean channel slope is  $0.007 \text{ m/m}$  and varying this parameter  $\pm 10\%$  produces a range of  $0.0063$  to  $0.0077 \text{ m m}^{-1}$ . For the Sulzigraben catchment, mean channel slope is  $0.07 \text{ m m}^{-1}$  and varying this parameter  $\pm 10\%$  produces a range of  $0.063$  to  $0.077 \text{ m m}^{-1}$ . The variability of mean channel slope for the Thur River catchment lies between  $0.00144$  and  $0.00176 \text{ m m}^{-1}$ , much smaller than for the other two catchments. As such, the relative deviation is the same, but the absolute deviation is greater for the Selwyn/Waikirikiriri River catchment and the Sulzigraben catchment, resulting in a higher variability of the modeled results. Although several hydrologic model calibration and validation concepts exist [88], no descriptive guidelines for sensitivity analyses are available. A relative deviation was chosen over a fixed value (e.g.,  $\pm 0.01 \text{ m m}^{-1}$  for channel slope) as we believe that measuring errors of  $\pm 10\%$  magnitude can occur in the field. In addition, determining mean channel width, mean channel slope, mean streambank angle and mean bend radius can be done rather easily and accurately in the field, but the exact determination of  $D_{50}$  is more time consuming and is spatially heterogeneous. Based on this, considerable effort is still needed to improve a more cost-effective method for the estimation of this parameter for practical applications. Further, median grain size is not the same on the surface of a streambank or riverbed as it is in depth. While the framework estimates erosion for static  $D_{50}$  in time,  $D_{50}$  is not static as it changes as soon as material is removed and mobilized sediment from upstream is deposited, as shown by Pasquale et al. [79] for the Thur River catchment. Their results show that the standard deviation of the observed  $D_{50}$  at the surface is approximately  $15 \text{ mm}$ , whereas the standard deviation at depths of  $40 \text{ cm}$  is approximately  $2 \text{ mm}$ . To take this effect into account, a probability-density function adapting  $D_{50}$  values during an erosion event could have a significant effect on the modeled results as  $D_{50}$  will most likely change during erosion events. In addition, regarding the simplicity of the framework: measuring  $D_{50}$  is rather time consuming. The inclusion of an empirically derived function to estimate  $D_{50}$  as a function of mean channel slope and mean channel width [89] could be considered and used to compare measured and estimated  $D_{50}$  values to find a suitable density function or to define permissible  $D_{50}$  values.

Quantitative information on how roots stabilize streambanks is important for civil engineering, geomorphology, ecology as well as forest and channel management. Modeling hydraulic bank erosion for vegetated and nonvegetated streambanks helps to define criteria on how to manage mountain and riparian forests. Results of modeled erosion show that the effects of roots mitigating hydraulic bank erosion range between  $0\%$  and  $100\%$  under specific channel and root conditions. Based on the results of the 37 study reaches, a susceptibility matrix to hydraulic bank erosion in relation to channel width and channel slope was proposed showing the stabilizing effects of roots. The results suggest that the stabilizing effects of roots are highest for channels with widths  $< 15.00 \text{ m}$  and slopes  $< 0.05 \text{ m m}^{-1}$ . Based on a GIS analysis using the ecological morphology data provided by the Swiss Federal Office for the Environment, these criteria correspond approximately to  $42\%$  of all Swiss torrents and streams. Considering the effects of roots (RAR in vertical direction) was validated at the Sulzigraben catchment. A sycamore maple with a DBH of  $36 \text{ cm}$  had a measured RAR of max.  $2.3\%$  at  $30 \text{ cm}$  depth and  $1\%$  at  $60 \text{ cm}$  depth—the point where erosion occurred and was modeled—standing  $2.50 \text{ m}$  away from the



streambank/water interface. Considering a RAR of 1% at a radial distance of 2.50 m away from the tree stem, the ideal riparian forest conditions for the Sulzigraben catchment to decrease the susceptibility of hydraulic bank erosion can be reached with a forest stand of 510 trees per hectare and a mean DBH of 36 cm. With continuous erosion, RAR increases, subsequently reducing hydraulic bank erosion. As such, the reduction of hydraulic bank erosion is dependent on RAR, rooting depth, the difference and modification of critical and applied shear stress and streambank height. As long as channel incision is not greater than rooting depth, roots have a stabilizing (positive) effect. If no roots are present at the area affected by the flow, roots have no or very little influence on erosion reduction (see Figure 13).



**Figure 13.** Streambank in the Zulgraben river catchment, Canton of Bern, Switzerland. In the lower area of the streambank, no roots are present. In this area, roots have no influence on reducing the susceptibility of hydraulic bank erosion. The black arrow indicates the flow direction. Source: Eric Gasser.

By using actual flood statistics for the Thur River catchment, the effects of roots on hydraulic bank erosion were investigated by changing the RAR (no roots, 0.1%, 1% and 2%) for discharge scenarios with different return periods (RP of 2, 5, 30, 100 and 300 years). The results suggest that with increasing RAR, cumulative erosion reduction increases in a somewhat linear way up to 17% for discharge scenarios of lower magnitudes (i.e., RP of two years). With increasing event magnitude, cumulative erosion reduction decreases and the stabilizing effects of roots decrease by up to a factor of 0.65. The results further suggest that the ideal mountain or riparian forest conditions with RAR values of 1% to 2% reduce hydraulic bank erosion between 5% and 11% for discharge scenarios with return periods of 100 to 300 years.

While roots stabilize streambanks and reduce the susceptibility of erosion, they can also increase streambank roughness affecting flow velocity and flow depth. Determining vegetated streambank roughness iteratively based on the approach presented in Van De Wiel [90] was not implemented in BankforNET as it intends to keep the framework simple with least input in order to perform. Roots certainly affect roughness coefficients and influence turbulences, but what the relative magnitude of this effect is and how it affects streambank erosion in return was not an objective of the present framework.

## 5. Conclusions

The framework as presented is the foundation of BankforNET, a simple one-dimensional and event-based model to assess the susceptibility of hydraulic bank erosion at the streambank toe for a given cross section considering the stabilizing effects of roots and intrinsic randomness that characterize the Shields entrainment parameter. The effects of roots are implemented by determining RAR as well

as rooting depth hereby adapting the streambank's critical shear stress. The preliminary results suggest that the framework predicts hydraulic bank erosion with reasonable accuracy. Considering the effects of roots, the results also suggest that hydraulic bank erosion is significantly reduced up to 14% for the Sulzigraben catchment with a RAR of 1%. Collecting data on erodibility parameters, RAR and rooting depths for different tree species and soil types would enable a better parametrization of the model. Therefore, future work should focus on further parametrization and calibration.

The susceptibility matrix presented in this article highlights conceptually how roots can reduce the susceptibility of hydraulic bank erosion based on geometric criteria: channel width and channel slope. The results suggest that stabilizing (positive) effects are highest for channels with widths < 15.00 m, longitudinal slopes < 0.05 m m<sup>-1</sup> and RAR of 1% to 2%, reducing the susceptibility of hydraulic bank erosion up to 100%. Channel and forest managers could use the susceptibility matrix to identify areas where roots have significant effects on decreasing the susceptibility of hydraulic bank erosion. Their efforts should then be focused on areas where vegetation effects (i.e., root density) are high or variable to adapt forest densities or to perform targeted afforestation. Reducing the susceptibility of streambank erosion is only possible if roots are present at the area affected by the flow. Therefore, the matrix is only valid if streambank height is smaller than the maximum average rooting depth.

BankforNET will be further expanded to estimate the spatially explicit susceptibility of hydraulic bank erosion at catchment scale by extrapolating the effects of roots using single-tree detection algorithms. This will allow the assessment of hydraulic bank erosion at catchment scale with and without the effects of roots and highlight where the protective role of forests against hydraulic bank erosion could be optimized. Additionally, the results of the model can be used to assess potential LW recruitment due to hydraulic bank erosion. In combination with the assessment of potential LW recruitment due to other processes, the results could help civil engineers to dimension culverts, bridges or LW retention rakes.

**Author Contributions:** Conceptualization, E.G. and M.S.; Methodology, E.G., M.S. and P.P.; Validation, E.G. and M.S.; Formal Analysis, E.G., L.D. and C.P.; Investigation, E.G. and M.S.; Writing-Original Draft Preparation, E.G. and M.S.; Writing-Review & Editing, E.G., M.S., L.D., P.P., C.P. and J.H.; Visualization, E.G. and M.S.; Supervision, M.S., L.D. and P.P.; Project Administration, M.S., C.P. and L.D.; Funding Acquisition, M.S. and C.P. All authors have read and agreed to the published version of the manuscript.

**Funding:** This research was funded by the Swiss Federal Office for the Environment FOEN (grant number 15.0018.PJ/O192-3229) and the New Zealand Ministry of Business, Innovation and Employment (grant number C09X1804).

**Conflicts of Interest:** The authors declare no conflict of interest.

## References

1. Winsemius, H.C.; Van Beek, L.P.H.; Jongman, B.; Ward, P.J.; Bouwman, A. A framework for global river flood risk assessments. *Hydrol. Earth Syst. Sci.* **2013**, *17*, 1871–1892. [[CrossRef](#)]
2. Berz, G.; Kron, W.; Loster, T.; Rauch, E.; Schimetschek, J.; Schmieder, J.; Siebert, A.; Smolka, A.; Wirtz, A. World map of natural hazards—A global view of the distribution and intensity of significant exposures. *Nat. Hazards* **2001**, *23*, 443–465. [[CrossRef](#)]
3. Julien, P.Y. *River Mechanics*; Cambridge University Press: Cambridge, UK, 2018.
4. Smith, R.D.; Buffington, J.M. Effects of large woody debris on channel unit distribution in southeast Alaska. In Proceedings of the Watershed 1991, U.S. Forest Service Conference, Juneau, Alaska, 16–17 April 1991.
5. Montgomery, D.R.; Buffington, J.M. Channel classification, prediction of channel response, and assessment of channel condition. In *Report TFW-SI-110-93-002 prepared for the SHAMW committee of the Washington State Timber, Fish & Wildlife Agreement*; University of Washington: Seattle, WA, USA, 24 June 1993; pp. 1–84.
6. Cohen, A.S.; Bills, R.; Cocquyt, C.Z.; Caljon, A.G. The impact of sediment pollution on biodiversity in Lake Tanganyika. *Conserv. Biol.* **1993**, *7*, 667–677. [[CrossRef](#)]
7. Piégay, H.; Darby, S.E.; Mosselman, E.; Surian, N. A review of techniques available for delimiting the erodible river corridor: A sustainable approach to managing bank erosion. *River Res. Appl.* **2005**, *21*, 773–789. [[CrossRef](#)]



8. Lijklema, L.; Koelmans, A.A.; Portielje, R. Water quality impacts of sediment pollution and the role of early diagenesis. *Water Sci. Technol.* **1993**, *28*, 1–12. [[CrossRef](#)]
9. Darby, S.E.; Trieu, H.Q.; Carling, P.A.; Sarkkula, J.; Koponen, J.; Kumm, M.; Conlan, I.; Leyland, J. A physically based model to predict hydraulic erosion of fine-grained riverbanks: The role of form roughness in limiting erosion. *J. Geophys. Res. Earth Surf.* **2010**, *115*. [[CrossRef](#)]
10. Piégay, H.; Thevenet, A.; Citterio, A. Input, storage and distribution of large woody debris along a mountain river continuum, the Drôme River, France. *Catena* **1999**, *35*, 19–39. [[CrossRef](#)]
11. Gregory, S.; Boyer, K.L.; Gurnell, A.M. Ecology and management of wood in world rivers. In *Proceedings of the International Conference of Wood in World Rivers (2000: Corvallis, Or.)*; American Fisheries Society: Bethesda, MD, USA, 2003.
12. Lassetre, N.S.; Kondolf, G.M. Large woody debris in urban stream channels: Redefining the problem. *River Res. Appl.* **2012**, *28*, 1477–1487. [[CrossRef](#)]
13. Wohl, E.; Scott, D.N. Wood and sediment storage and dynamics in river corridors. *Earth Surf. Process. Landf.* **2017**, *42*, 5–23. [[CrossRef](#)]
14. Janes, V.; Holman, I.; Birkinshaw, S.; O'Donnell, G.; Kilsby, C. Improving bank erosion modelling at catchment scale by incorporating temporal and spatial variability. *Earth Surf. Process. Landf.* **2018**, *43*, 124–133. [[CrossRef](#)]
15. Ruiz-Villanueva, V.; Mazzorana, B.; Bladé, E.; Bürkli, L.; Iribarren-Anacona, P.; Mao, L.; Nakamura, F.; Ravazzolo, D.; Rickenmann, D.; Sanz-Ramos, M.; et al. Characterization of wood-laden flows in rivers. *Earth Surf. Process. Landf.* **2019**, *44*, 1694–1709. [[CrossRef](#)]
16. Simon, A.; Collison, A.J.C. Quantifying the mechanical and hydrological effects of riparian vegetation on streambank stability. *Earth Surf. Process. Landf.* **2002**, *27*, 527–546. [[CrossRef](#)]
17. Pollen, N.; Simon, A. Estimating the mechanical effects of riparian vegetation on stream bank stability using a fiber bundle model. *Water Resour. Res.* **2005**, *41*, W07025. [[CrossRef](#)]
18. Docker, B.B.; Hubble, T.C.T. Quantifying root-reinforcement of river bank soils by four Australian tree species. *Geomorphology* **2008**, *100*, 401–418. [[CrossRef](#)]
19. Osborne, L.L.; Kovacic, D.A. Riparian vegetated buffer strips in water-quality restoration and stream management. *Freshw. Biol.* **1993**, *29*, 243–258. [[CrossRef](#)]
20. Dosskey, M.G.; Vidon, P.; Gurwick, N.P.; Allan, C.J.; Duval, T.P.; Lowrance, R. The role of riparian vegetation in protecting and improving chemical water quality in streams. *JAWRA J. Am. Water Resour. Assoc.* **2010**, *46*, 261–277. [[CrossRef](#)]
21. Fetherston, K.L.; Naiman, R.J.; Bilby, R.E. Large woody debris, physical process, and riparian forest development in montane river networks of the Pacific Northwest. *Geomorphology* **1995**, *13*, 133–144. [[CrossRef](#)]
22. Abbe, T.B.; Montgomery, D.R. Large woody debris jams, channel hydraulics and habitat formation in large rivers. *Regul. Rivers Res. Manag.* **1996**, *12*, 201–221. [[CrossRef](#)]
23. Aarts, B.G.; Van Den Brink, F.W.; Nienhuis, P.H. Habitat loss as the main cause of the slow recovery of fish faunas of regulated large rivers in Europe: The transversal floodplain gradient. *River Res. Appl.* **2004**, *20*, 3–23. [[CrossRef](#)]
24. Wohl, E. Bridging the gaps: An overview of wood across time and space in diverse rivers. *Geomorphology* **2016**, *279*, 3–26. [[CrossRef](#)]
25. Wohl, E.; Angermeier, P.L.; Bledsoe, B.; Kondolf, G.M.; MacDonnell, L.; Merritt, D.M.; Palmer, M.A.; LeRoy Poff, N.; Tarboton, D. River restoration. *Water Resour. Res.* **2005**, *41*. [[CrossRef](#)]
26. Partheniades, E. Erosion and deposition of cohesive soils. *J. Hydraul. Div.* **1965**, *91*, 105–139.
27. Hanson, G.J.; Simon, A. Erodibility of cohesive streambeds in the loess area of the midwestern USA. *Hydrol. Process.* **2001**, *15*, 23–38. [[CrossRef](#)]
28. Stecca, G.; Measures, R.; Hicks, D.M. A framework for the analysis of noncohesive bank erosion algorithms in morphodynamic modeling. *Water Resour. Res.* **2017**, *53*, 6663–6686. [[CrossRef](#)]
29. Rinaldi, M.; Darby, S.E. Modelling river-bank-erosion processes and mass failure mechanisms: Progress towards fully coupled simulations. *Gravel-Bed Rivers VI: Form Process Understanding to River Restoration. Dev. Earth Surf. Process.* **2007**, *11*, 213–239.
30. Lawler, D.M. Process dominance in bank erosion systems. In *Lowland Floodplain Rivers*; Carling, P., Petts, G.E., Eds.; Wiley: Chichester, UK, 1992; pp. 117–143.

31. Couper, P.R.; Maddock, I.P. Subaerial river bank erosion processes and their interaction with other bank erosion mechanisms on the River Arrow, Warwickshire, UK. *Earth Surf. Process. Landf.* **2001**, *26*, 631–646. [\[CrossRef\]](#)
32. Wynn, T.M.; Mostaghimi, S.; Alphin, E.F. The effects of vegetation on stream bank erosion. In *Proceedings of the 2004 ASAE Annual Meeting*; American Society of Agricultural and Biological Engineers: Ottawa, ON, Canada, 2004.
33. Hubble, T.C.T.; Docker, B.B.; Rutherford, I.D. The role of riparian trees in maintaining riverbank stability: A review of Australian experience and practice. *Ecol. Eng.* **2010**, *36*, 292–304. [\[CrossRef\]](#)
34. Pollen-Bankhead, N.; Simon, A. Hydrologic and hydraulic effects of riparian networks on streambank stability: Is mechanical root reinforcement the whole story? *Geomorphology* **2010**, *116*, 353–362. [\[CrossRef\]](#)
35. Julian, P.J.; Torres, R. Hydraulic erosion of cohesive riverbanks. *Geomorphology* **2006**, *76*, 193–206. [\[CrossRef\]](#)
36. Smith, H.G.; Spiekermann, R.; Dymond, J.; Basher, L. Predicting spatial patterns in riverbank erosion for catchment sediment budgets. *N. Z. J. Mar. Freshwater Res.* **2019**, *53*, 338–362. [\[CrossRef\]](#)
37. Thorne, C.R. Processes and mechanisms of river bank erosion. In *Gravel-Bed Rivers*; Hey, R.D., Bathurst, J.C., Thorne, C.R., Eds.; Wiley: Chichester, UK, 1982; pp. 227–271.
38. Fischenich, C. *Stability Thresholds for Stream Restoration Materials*; USAE Engineering Research and Development Center, Environmental Lab: Vicksburg, MS, USA, 2001.
39. Liu, D.; Diplas, P.; Fairbanks, J.D.; Hodges, C.C. An experimental study of flow through rigid vegetation. *J. Geophys. Res. Earth Surf.* **2008**, *113*. [\[CrossRef\]](#)
40. Nepf, H.; Ghisalberti, M. Flow and transport in channels with submerged vegetation. *Acta Geophys.* **2008**, *56*, 753–777. [\[CrossRef\]](#)
41. Magilligan, F.J. Thresholds and the spatial variability of flood power during extreme floods. *Geomorphology* **1992**, *5*, 373–390. [\[CrossRef\]](#)
42. Pasquale, N.; Perona, P. Experimental assessment of riverbed sediment reinforcement by vegetation roots. In *River Flow 2014*; Crc Press-Taylor & Francis Group: Leiden, The Netherlands, 2014; No. CONF, pp. 553–561.
43. Bloemer, S.; Fernandes, J.P.; Florineth, F.; Geitz, P.; Gerstgraser, C.; Graf, F.; Hacker, E.; Johannsen, R.; Kovalev, N.; Markart, G.; et al. European Guidelines for Soil and Water Bioengineering. European Federation for Soil and Water Bioengineering: 2015. Available online: <http://hdl.handle.net/10174/14589> (accessed on 22 March 2020).
44. Van de Wiel, M.J.; Darby, S.E. A new model to analyse the impact of woody riparian vegetation on the geotechnical stability of riverbanks. *Earth Surf. Process. Landf.* **2007**, *32*, 2185–2198. [\[CrossRef\]](#)
45. Langendoen, E.J.; Lowrance, R.R.; Simon, A. Assessing the impact of riparian processes on streambank stability. *Ecohydrology* **2009a**, *2*, 360–369. [\[CrossRef\]](#)
46. Simon, A.; Curini, A.; Darby, S.E.; Langendoen, E.J. Bank and near-bank processes in an incised channel. *Geomorphology* **2000**, *35*, 193–217. [\[CrossRef\]](#)
47. Pollen, N. Temporal and spatial variability in root reinforcement of streambanks: Accounting for soil shear strength and moisture. *Catena* **2007**, *69*, 197–205. [\[CrossRef\]](#)
48. Klavon, K.; Fox, G.; Guertault, L.; Langendoen, E.; Enlow, H.; Miller, R.; Khanal, A. Evaluating a process-based model for use in streambank stabilization: Insights on the Bank Stability and Toe Erosion Model (BSTEM). *Earth Surf. Process. Landf.* **2017**, *42*, 191–213. [\[CrossRef\]](#)
49. Lowrance, R.; Altier, L.S.; Williams, R.G.; Inamdar, S.P.; Sheridan, J.M.; Bosch, D.D.; Hubbard, R.K.; Thomas, D.L. REMM: The riparian ecosystem management model. *J. Soil Water Conserv.* **2000**, *55*, 27–34.
50. Langendoen, E.J.; Alonso, C.V. Modeling the evolution of incised streams: I. Model formulation and validation of flow and streambed evolution components. *J. Hydraul. Eng.* **2009b**, *134*, 749–762. [\[CrossRef\]](#)
51. Langendoen, E.J.; Simon, A. Modeling the evolution of incised streams. II: Streambank erosion. *J. Hydraul. Eng.* **2008a**, *134*, 905–915. [\[CrossRef\]](#)
52. Langendoen, E.J.; Wells, R.R.; Thomas, R.E.; Simon, A.; Bingner, R.L. Modeling the evolution of incised streams. iii: Model application. *J. Hydraul. Eng.* **2009b**, *135*, 476–486. [\[CrossRef\]](#)
53. Neitsch, S.L.; Arnold, J.G.; Kiniry, J.R.; Williams, J.R.; King, K.W. *Soil and Water Assessment Tool (SWAT): Theoretical Documentation, Version 2000*; Texas Water Resources Institute: College Station, TX, USA, 2002; TWRI Report TR-191.
54. Gassman, P.W.; Reyes, M.R.; Green, C.H.; Arnold, J.G. The soil and water assessment tool: Historical development, applications, and future research directions. *Trans. ASABE* **2007**, *50*, 1211–1250. [\[CrossRef\]](#)

55. Narasimhan, B.; Allen, P.M.; Coffman, S.V.; Arnold, J.G.; Srinivasan, R. Development and testing of a physically based model of streambank erosion for coupling with a basin-scale hydrologic model SWAT. *JAWRA J. Am. Water Resour. Assoc.* **2017**, *53*, 344–364. [\[CrossRef\]](#)
56. Wilkinson, S.N.; Prosser, I.P.; Rustomji, P.; Read, A.M. Modelling and testing spatially distributed sediment budgets to relate erosion processes to sediment yields. *Environ. Model. Softw.* **2009**, *24*, 489–501. [\[CrossRef\]](#)
57. Wilkinson, S.N.; Dougall, C.; Kinsey-Henderson, A.E.; Searle, R.D.; Ellis, R.J.; Bartley, R. Development of a time-stepping sediment budget model for assessing land use impacts in large river basins. *Sci. Total Environ.* **2014**, *468*, 1210–1224. [\[CrossRef\]](#)
58. Hanson, G.J.; Cook, K.R. Development of excess shear stress parameters for circular jet testing. In Proceedings of the American Society of Agricultural Engineers International Meeting, Minneapolis, Minnesota, 10–14 August 1997; Paper no. 972227, pp. 1–21.
59. Clark, L.A.; Wynn, T.M. Methods for determining streambank critical shear stress and soil erodibility: Implications for erosion rate predictions. *Trans. ASABE* **2007**, *50*, 95–106. [\[CrossRef\]](#)
60. Fortier, S.; Scobey, F.C. Permissible canal velocities. *Trans. Am. Soc. Civ. Eng.* **1926**, *89*, 940–956.
61. Shields, A. Anwendung der Aehnlichkeitsmechanik und der Turbulenzforschung auf die Geschiebebewegung. Ph.D. Thesis, Technical University Berlin, Berlin, Germany, 1936.
62. Petit, F.; Houbrechts, G.; Peeters, A.; Hallot, E.; Van Campenhout, J.; Denis, A.C. Dimensionless critical shear stress in gravel-bed rivers. *Geomorphology* **2015**, *250*, 308–320. [\[CrossRef\]](#)
63. Mostafa, T.S.; Imran, J.; Chaudhry, M.H.; Kahn, I.B. Erosion resistance of cohesive soils. *J. Hydraul. Res.* **2008**, *46*, 777–787. [\[CrossRef\]](#)
64. Berenbrock, C.; Tranmer, A.W. Simulation of flow, sediment transport, and sediment mobility of the Lower Coeur d'Alene River, Idaho. In *U.S. Geological Survey Scientific Investigations Report 2008-5093*; US Geological Survey: Reston, VA, USA, 2008; pp. 1–164.
65. Bunte, K.; Abt, S.R.; Swingle, K.W.; Cenderelli, D.A.; Schneider, J.M. Critical Shields values in coarse-bedded steep streams. *Water Resour. Res.* **2013**, *49*, 7427–7447. [\[CrossRef\]](#)
66. Bischetti, G.B.; Chiaradia, E.A.; Simonato, T.; Spezialia, B.; Vitali, B.; Vullo, P.; Zocco, A. Root strength and root area ratio of forest species in Lombardy (Northern Italy). *Plant Soil* **2005**, *278*, 11–22. [\[CrossRef\]](#)
67. Schwarz, M.; Cohen, D.; Or, D. Root-soil mechanical interactions during pullout and failure of root bundles. *J. Geophys. Res. Earth Surf.* **2010**, *115*. [\[CrossRef\]](#)
68. Tron, S.; Perona, P.; Gorla, L.; Schwarz, M.; Laio, F.; Ridolfi, L. The signature of randomness in riparian plant root distributions. *Geophys. Res. Lett.* **2015**, *42*, 7098–7106. [\[CrossRef\]](#)
69. Caflisch, F. Wurzelentwicklung und -Verstärkung von Grauerlen in Ingenieurbiologischen Massnahmen. Eine Fallstudie im Gebiet Arieschbach, Fideris (GR). Bachelor Thesis, Bern University of Applied Sciences, Zollikofen, Switzerland, 2015; pp. 1–86.
70. Bischetti, G.B.; Chiaradia, E.A.; Epis, T.; Morlotti, E. Root cohesion of forest species in the Italian Alps. *Plant Soil* **2009**, *324*, 71–89. [\[CrossRef\]](#)
71. Abdi, E.; Majnounian, B.; Rahimi, H.; Zobeiri, M.; Mashayekhi, Z.; Yosefzadeh, H. A comparison of root distribution of three hardwood species grown on a hillside in the Caspian forest, Iran. *J. For. Res.* **2010**, *15*, 99–107. [\[CrossRef\]](#)
72. Naghdi, R.; Maleki, S.; Abdi, E.; Mousavi, R.; Nikooy, M. Assessing the effect of *Alnus* roots on hillslope stability in order to use in soil bioengineering. *J. For. Sci.* **2013**, *59*, 417–423. [\[CrossRef\]](#)
73. Kölla, E. Estimating flood peaks from small rural catchments in Switzerland. *J. Hydrol.* **1987**, *95*, 203–225. [\[CrossRef\]](#)
74. Marchi, L.; Borga, M.; Preciso, E.; Gaume, E. Characterisation of selected extreme flash floods in Europe and implications for flood risk management. *J. Hydrol.* **2010**, *394*, 118–133. [\[CrossRef\]](#)
75. Soil Conservation Service SCS. *National Engineering Handbook, Section 4*; U.S. Department of Agriculture: Washington, DC, USA, 1972.
76. Schirmer, M.; Luster, J.; Linde, N.; Perona, P.; Mitchell, E.A.; Barry, D.A.; Hollender, J.; Cirpka, O.A.; Schneider, P.; Vogt, T.; et al. Durisch-Kaiser, Morphological, hydrological, biogeochemical and ecological changes and challenges in river restoration—The Thur River case study. *Hydrol. Earth Syst. Sci.* **2014**, *18*, 2449–2462. [\[CrossRef\]](#)
77. Schälchli, U.; Abbegg, J.; Hunzinger, L. Geschiebestudie Thur und Einzugsgebiet. In *Ämter für Umwelt der Kantone Zürich; Thurgau: Appenzell und St. Gallen, Switzerland*, 2005.

78. Cattaneo, G. Hydrodynamic Simulations and Bank Stability Analysis of a Morphodynamically Active Restored River Corridor (Thur River, Switzerland). Master's Thesis, École polytechnique fédérale de Lausanne EPFL, Lausanne, Switzerland, July 2012.
79. Pasquale, N.; Perona, P.; Wombacher, A.; Burlando, P. Hydrodynamic model calibration from pattern recognition of non-orthorectified terrestrial photographs. *Comput. Geosci.* **2014**, *62*, 160–167. [\[CrossRef\]](#)
80. Swiss Federal Office for the Environment: Discharge and water level measurements for the river Thur–Andelfingen. Available online: <https://www.hydrodaten.admin.ch/en/2044.html> (accessed on 2 May 2019).
81. Hunziker, G. Hochwasser vom 7. Juni 2015 in der Zulg. In *Ereignisanalyse*; Hunziker Gefahrenmanagement: Kerzers, Switzerland, 2015; pp. 1–36.
82. Fehr, R. Einfache Bestimmung der Korngrößenverteilung von geschiebmaterial mit Hilfe der Linienzahlanalyse. *Schweiz. Ing. Und Archt.* **1987**, *38*, 1104–1109.
83. Wohl, E.E.; Wilcox, A. Channel geometry of mountain streams in New Zealand. *J. Hydrol.* **2005**, *300*, 252–266. [\[CrossRef\]](#)
84. Gasser, E.; Schwarz, M.; Simon, A.; Perona, P.; Phillips, C.; Hübl, J.; Dorren, L. A review of modeling the effects of vegetation on large wood recruitment processes in mountain catchments. *Earth-Sci. Rev.* **2019**, *194*, 350–373. [\[CrossRef\]](#)
85. ASTM. *Standard Test Method for Erodibility Determination of Soil in the Field or in the Laboratory by the Jet Index Method*; D 5852-00; ASTM: West Conshohocken, PA, USA, 1999; pp. 1–6.
86. Wynn, T.; Mostaghimi, S. The effects of vegetation and soil type on streambank erosion, southwestern Virginia, USA. *J. Am. Water Resour. Assoc.* **2006**, *42*, 69–82. [\[CrossRef\]](#)
87. Enlow, H.; Fox, G.; Guertault, L. Watershed variability in streambank erodibility and implications for erosion prediction. *Water* **2017**, *9*, 605. [\[CrossRef\]](#)
88. Yuan, Y.; Khare, Y.; Wang, X.; Parajuli, P.B.; Kisekka, I.; Finsterle, S. Hydrologic and water quality models: Sensitivity. *Trans. ASABE* **2015**, *58*, 1721–1744.
89. Golden, L.A.; Springer, G.S. Channel geometry, median grain size, and stream power in small mountain streams. *Geomorphology* **2006**, *78*, 64–76. [\[CrossRef\]](#)
90. Van De Wiel, M.J. Numerical Modelling of Channel Adjustment in Alluvial Meandering Rivers with Riparian Vegetation. Ph.D. Thesis, University of Southampton, Southampton, UK, 2003.



© 2020 by the authors. Licensee MDPI, Basel, Switzerland. This article is an open access article distributed under the terms and conditions of the Creative Commons Attribution (CC BY) license (<http://creativecommons.org/licenses/by/4.0/>).